Available online at www.sciencedirect.com

SCIENCE DIRECT

Solid State Ionics 172 (2004) 491–494

SOLID STATE IONICS

www.elsevier.com/locate/ssi

Single-crystal X-ray structure analysis of the low temperature form of $LiMn_2O_4$

Junji Akimoto*, Yasuhiko Takahashi, Norihito Kijima, Yoshito Gotoh

National Institute of Advanced Industrial Science and Technology (AIST), 1-1-1 Higashi, Tsukuba, Ibaraki 305-8565, Japan

Received 09 November 2003; received in revised form 30 January 2004; accepted 30 January 2004

Abstract

Crystal structure of the low temperature form of $LiMn_2O_4$ has been successfully determined by using single-crystal X-ray diffraction data at 130 K. It belongs to the orthorhombic system, space group *Fddd* with $a = 24.750(3)$ Å, $b = 24.801(2)$ Å, $c = 8.1903(9)$ Å, and $V = 5027.4(9)$ Å^3. The structure, including anisotropic displacement parameters for each atom, was refined to the conventional values $R1 = 5.58\%$, $wR2 = 7.16\%$, and $S = 1.180$ for 8082 independent reflections. The oxygen sublattice deformation toward the [1 1 0] direction in the low temperature form is clearly observed at 130 K. The structural phase transition around 280 and 320 K was precisely examined by differential scanning calorimetry (DSC) and single-crystal X-ray diffraction measurements using the single-crystal samples.

PACS: 61.50.Ks; 61.10.Nz; 81.10.Dn; 81.30.−t
Keywords: Lithium-ion battery; $LiMn_2O_4$; Spinel; Single-crystal X-ray diffraction; Low-temperature form; Structural phase transition; Structure analysis

1. Introduction

In the past few years, the lithium transition metal oxides such as $LiCoO_2$, $LiNiO_2$, and $LiMn_2O_4$ have been extensively studied as cathode materials for rechargeable lithium-ion batteries, since these can be reversibly deintercalated and reintercalated by lithium ions at high potential. Recently, special attention has been paid to the spinel-type lithium manganates due to its economical and environmental advantages [1]. $LiMn_2O_4$ presents a first order structural transition around room temperature [2]. Above the transition temperature, it has the cubic spinel structure with $Fd\bar{3}m$ space group. The crystal structure of the low temperature form has been recently investigated with the orthorhombic symmetry and *Fddd* space group by using the neutron powder diffraction method [3]. However, the mechanism of structural transition has not been clarified yet.

Recently, we have succeeded in the synthesis of $LiMn_2O_4$ single crystals by a flux method [4,5], and revealed the precise crystal and electronic structures of the cubic $LiMn_2O_4$ [4,6]. In this paper, we demonstrate the precise crystal structure determination of low temperature form of $LiMn_2O_4$ by single-crystal X-ray diffraction method.

2. Experimental and results

2.1. Crystal characterization

Single crystals of the stoichiometric $LiMn_2O_4$ were grown by a flux method, as reported recently [4–7]. Black, octahedral single crystals of about $0.20 \times 0.20 \times 0.20$ mm^3 in the maximum size were obtained. Chemical analysis using selected single crystals, carried out by SEM–EDX (JEOL JSM-5400) and inductively coupled plasma (ICP) spectroscopy, confirmed the stoichiometric chemical composition; the result was consistent with that of the structure refinement. The density of $LiMn_2O_4$, measured using a few single-crystal specimens and Clerici's heavy fluid, is 4.29 ± 0.01 g/cm^3 at 300 K; this value is consistent with the calculated value (4.286 g/cm^3). This fact allows one to conclude that the present $LiMn_2O_4$

* Corresponding author. Tel./fax: +81-29-861-9214.
E-mail address: j.akimoto@aist.go.jp (J. Akimoto).

0167-2738/$ - see front matter © 2004 Elsevier B.V. All rights reserved.
doi:10.1016/j.ssi.2004.01.051

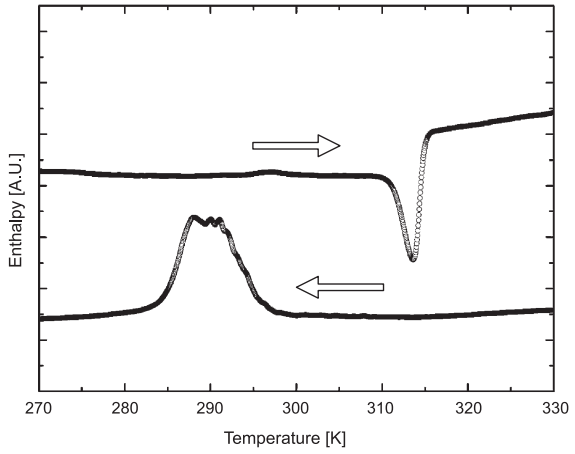

Fig. 1. DSC curves of the $LiMn_2O_4$ single crystals with heating and cooling rates of 5 K/min.

single crystals have no oxygen deficiency within the experimental error.

The phase transition was confirmed using differential scanning calorimetry (DSC) measurements (SEIKO DSC6200). Fig. 1 shows the DSC curves of the present $LiMn_2O_4$ single-crystal samples (9.51 mg). The transitions were observed around 280 and 320 K; the result is well consistent with those reported using powder samples [3,8,9].

The crystal symmetry and structural data were examined by the precession camera and an automated four-circle X-ray diffractometer (Rigaku AFC-7S), respectively. Temperature dependence of the lattice parameters for $LiMn_2O_4$ single crystals between 100 and 330 K was precisely investigated on the four-circle diffractometer using a nitrogen gas flow cryostat. The structural phase transition around 300 K has been also confirmed by the temperature dependence of integrated peak intensity for the superlattice (2/3 10/3 0) reflection observed in the low temperature orthorhombic form (Fig. 2).

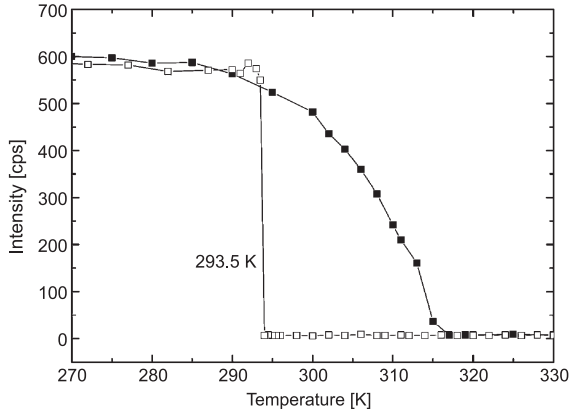

Fig. 2. Thermal hysteresis of the peak intensity for the superlattice (2/3 10/3 0) spot observed by single-crystal X-ray diffraction method.

Table 1
Experimental and crystallographic data for $LiMn_2O_4$ at 130 K

Temperature [K]	130
Crystal system	Orthorhombic
Space group	*Fddd*
a [Å]	24.750(3)
b [Å]	24.801(2)
c [Å]	8.1903(9)
V [Å^3]	5027.4(9)
Z	72
Crystal size [mm]	0.15 × 0.15 × 0.15
Max. 2θ [°]	110
Index ranges	$-56 \le h \le 49$, $-57 \le k \le 49$, $-18 \le l \le 3$
Reflection collected	13,360
Independent reflections	8082 [$R_{int} = 0.0523$]
Absorption correction	Gaussian integration
Max. and min. transmission	0.4076 and 0.3223
Refinement method	Full-matrix least-squares on F^2
Data/restraints/parameters	8082:0:148
Goodness-of-fit on F^2	1.180
Final *R* indices [$I > 2\sigma(I)$]	$R1 = 0.0558$, $wR2 = 0.0716$
R indices (all data)	$R1 = 0.1892$, $wR2 = 0.0851$
Largest diff. peak and hole [e/Å^3]	2.381 and −2.892

2.2. Structure analysis

A small octahedral crystal of $LiMn_2O_4$, 0.15 × 0.15 × 0.15 mm in size, was used for the intensity data collection. The intensity data were collected by the $2\theta - \omega$ scan mode with a scan rate of 2 °/min at 130, 200, and 330 K on the four-circle diffractometer (operating conditions: 50 kV, 30 mA) using graphite-monochromatized Mo*K*α radiation ($\lambda = 0.71073$ Å). Absorption corrections were performed using the XTAL3.4 program [10].

As previously reported by us [4,5], the crystal was in the orthorhombic symmetry at low temperatures with the $3a \times 3a \times a$ superstructure, and splitting of main Bragg

Table 2
Atomic coordinates and equivalent isotropic displacement parameters for $LiMn_2O_4$ at 130 K

Atom	Site	*x*	*y*	*z*	U_{eq} (Å^2)
Li1	*8a*	1/8	1/8	1/8	0.012(3)
Li2	*16f*	3/8	0.2126(3)	3/8	0.008(3)
Li3	*16e*	0.2058(4)	3/8	3/8	0.012(3)
Li4	*32h*	0.2905(4)	0.2940(4)	0.1243(10)	0.0104(12)
Mn1	*16d*	1/4	1/4	1/2	0.00514(13)
Mn2	*32h*	0.08104(3)	0.08503(2)	0.50112(9)	0.00533(8)
Mn3	*32h*	0.08401(3)	0.33053(3)	0.24981(11)	0.00508(8)
Mn4	*32h*	0.25333(3)	0.16804(2)	0.24506(10)	0.00454(10)
Mn5	*32h*	0.16668(2)	0.24427(2)	0.24440(9)	0.00397(9)
O1	*32h*	0.17443(11)	0.16824(10)	0.2622(4)	0.0065(4)
O2	*32h*	0.07891(12)	0.00767(10)	0.4804(5)	0.0062(4)
O3	*32h*	0.07874(13)	0.33225(11)	0.4820(5)	0.0088(5)
O4	*32h*	0.25205(14)	0.17260(9)	0.4766(5)	0.0089(5)
O5	*32h*	0.00650(11)	0.00675(9)	0.2381(4)	0.0072(4)
O6	*32h*	0.25636(12)	0.09017(9)	0.2383(5)	0.0066(5)
O7	*32h*	0.16256(12)	0.32346(10)	0.2363(5)	0.0074(5)
O8	*32h*	0.08990(10)	0.24413(9)	0.2345(5)	0.0056(4)
O9	*32h*	0.08369(16)	0.16162(10)	0.5156(4)	0.0135(6)

Table 3
Anisotropic displacement parameters (Å^2) for $LiMn_2O_4$ at 130 K

Atom	U_{11}	U_{22}	U_{33}	U_{23}	U_{13}	U_{12}
Li1	0.006(6)	0.010(5)	0.021(10)	0	0	0
Li2	0.004(4)	0.007(3)	0.011(7)	0	−0.001(5)	0
Li3	0.011(5)	0.015(5)	0.010(7)	−0.003(5)	0	0
Li4	0.016(4)	0.008(2)	0.007(3)	0.005(3)	0.005(4)	−0.001(2)
Mn1	0.0058(3)	0.00463(19)	0.0050(3)	−0.0005(3)	−0.0003(3)	0.0000(2)
Mn2	0.00566(16)	0.00565(14)	0.0047(2)	−0.00013(19)	−0.00049(19)	−0.00100(14)
Mn3	0.00379(14)	0.00665(13)	0.0048(2)	−0.00023(17)	0.00046(18)	0.00003(13)
Mn4	0.00455(17)	0.00485(11)	0.0042(3)	−0.0001(2)	0.00119(17)	−0.00006(13)
Mn5	0.00359(15)	0.00437(13)	0.0039(2)	0.00002(16)	0.0000(2)	0.00028(12)
O1	0.0051(8)	0.0060(6)	0.0086(10)	−0.0027(10)	−0.0012(9)	−0.0007(6)
O2	0.0085(9)	0.0054(6)	0.0048(11)	0.0015(8)	−0.0026(10)	0.0021(6)
O3	0.0055(9)	0.0141(9)	0.0068(11)	0.0037(11)	−0.0007(10)	0.0003(8)
O4	0.0153(11)	0.0045(7)	0.0067(13)	0.0005(8)	−0.0047(11)	0.0022(7)
O5	0.0063(8)	0.0074(7)	0.0079(12)	−0.0034(9)	0.0021(10)	−0.0001(6)
O6	0.0059(8)	0.0066(7)	0.0074(12)	−0.0018(9)	−0.0006(10)	0.0003(7)
O7	0.0044(9)	0.0113(8)	0.0064(12)	−0.0011(9)	−0.0003(10)	−0.0002(7)
O8	0.0076(9)	0.0062(7)	0.0029(9)	0.0000(8)	−0.0002(9)	−0.0018(6)
O9	0.0256(14)	0.0062(7)	0.0087(12)	0.0004(10)	−0.0001(17)	0.0011(9)

reflections was clearly observed because of the formation of mainly three twin components inside the crystal. However, by slow cooling rate of 0.05 K/min, we have successfully measured the intensity data of mainly single domain specimen with the orthorhombic symmetry in the present study.

In the structure analysis of low temperature form that followed, the reported space group of *Fddd*, confirmed by successful refinement, was adopted. The refinement was initiated using the reported coordination model [3]. Further oxygen population refinements were applied for all oxygen sites. However, such a deficient model did not improve the *R* values. This is consistent with the density measurement result. Finally, the structure was refined to $R1 = 5.58\%$ and $wR2 = 7.16\%$, and $S = 1.180$ for 8082 reflections using the SHELX-97 program [11]. A summary of the crystallographic and experimental data is given in Table 1. The final atomic coordinates and displacement parameters are given in Tables 2 and 3.

3. Structure description and discussion

The crystal structure of $LiMn_2O_4$ at 330 K was refined at first using the normal spinel atomic coordinates ($Fd\bar{3}m$ space group; Li at the *8a* site, Mn at the *16d* site, and O at the *32e* site), and the obtained structural parameters ($a = 8.2455(7)$ Å, $x(O) = 0.26341(14)$, final $R1 = 2.49\%$ using 206 reflections) are in good agreement with the previous reports [3,4,6]. On the other hand, the structure of the low temperature form at 130 K successfully converged to sufficiently good *R* values, including anisotropic displacement parameters for each atom. The refined structural parameters and bond distances were in good agreement with the original reports by neutron powder data [3] but

Table 4
Selected bond distances (Å) and bond valence sums (BVS) for $LiMn_2O_4$ at 130 K

Li1	-O1	1.977(3)	Mn2	-O9	1.904(3)
	-O1^{I}	1.977(3)		-O9^{ix}	1.914(3)
	-O1^{ii}	1.977(3)		-O2	1.927(3)
	-O1^{iii}	1.977(3)		-O1^{i}	1.963(4)
	mean	1.977		-O4^{i}	2.075(4)
	BVS	+1.00		-O9^{i}	2.115(4)
				mean	1.983
Li2	-O3^{iv}	1.980(6)		BVS	+3.36
	-O3^{v}	1.980(6)			
	-O2^{vi}	1.989(6)	Mn3	-O3	1.906(4)
	-O2^{vii}	1.989(6)		-O6^{x}	1.939(3)
	mean	1.985		-O7^{ii}	1.944(4)
	BVS	+0.98		-O7	1.955(3)
				-O8	2.151(2)
Li3	-O4^{v}	1.989(7)		-O3^{viii}	2.172(3)
	-O4^{vii}	1.989(7)		mean	2.011
	-O7	2.017(7)		BVS	+3.16
	-O7^{viii}	2.017(7)			
	mean	2.003	Mn4	-O3^{iv}	1.869(3)
	BVS	+0.94		-O5^{i}	1.882(3)
				-O4	1.900(4)
Li4	-O9^{iv}	1.922(9)		-O6^{iii}	1.924(4)
	-O8^{iv}	1.924(10)		-O6	1.934(2)
	-O5^{i}	1.950(8)		-O1	1.958(3)
	-O6^{vii}	1.974(10)		mean	1.911
	mean	1.943		BVS	+3.93
	BVS	+1.10			
			Mn5	-O8^{ii}	1.882(4)
Mn1	-O4	1.930(2)		-O1	1.901(3)
	-O4^{v}	1.930(2)		-O5^{i}	1.902(3)
	-O2^{i}	1.969(3)		-O8	1.902(2)
	-O2^{vi}	1.969(3)		-O2^{i}	1.936(4)
	-O5^{vi}	2.157(4)		-O7	1.968(2)
	-O5^{i}	2.157(4)		mean	1.915
	mean	2.019		BVS	+3.88
	BVS	+3.08			

Symmetry transformations used to generate equivalent atoms: (i) $-x+1/4, -y+1/4, z$; (ii) $-x+1/4, y, -z+1/4$; (iii) $x, -y+1/4, -z+1/4$; (iv) $x+1/4, -y+1/2, z-1/4$; (v) $-x+1/2, -y+1/2, -z+1$; (vi) $x+1/4, y+1/4, -z+1$; (vii) $-x+1/2, y+1/4, z-1/4$; (viii) $x, -y+3/4, -z+3/4$; (ix) $x, -y+1/4, -z+5/4$; (x) $x-1/4, y+1/4, -z+1/2$.

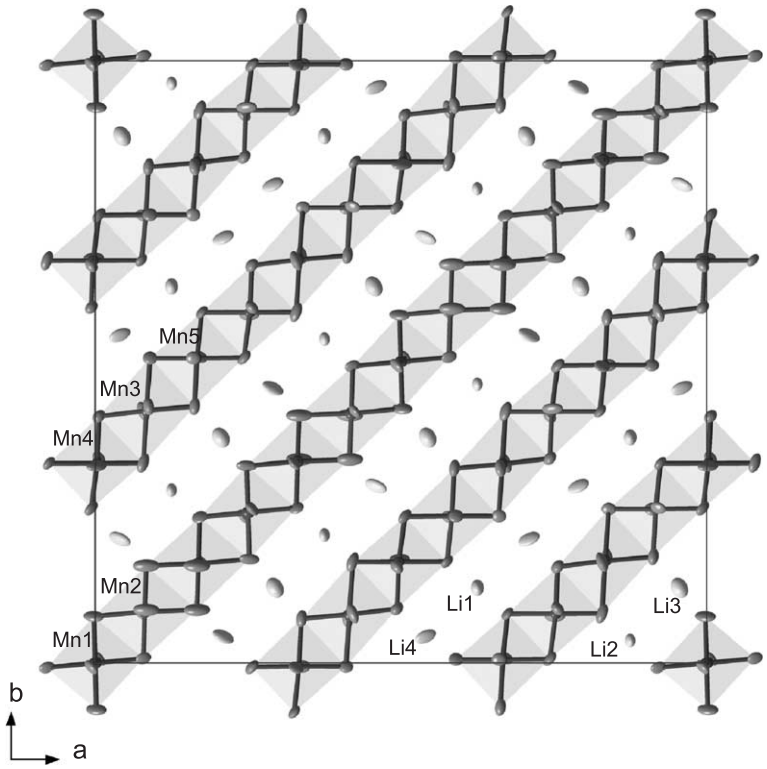

Fig. 3. Octahedral representations for the crystal structure of low temperature form in the range of $\sim 1/4 < z < \sim 3/4$. The Li, Mn, and O atoms are drawn as light grey, black, and dark grey balls, respectively. Displacement ellipsoids are scaled to include 95% probability.

with higher accuracy (Tables 2–4). The valence states for five Mn atoms were estimated by the bond valence [12]. As shown in Fig. 3, the oxygen sublattice deformation toward the [1 1 0] direction in the low temperature form is clearly visible in comparison with the orderly arrangement in the cubic spinel structure. This fact may lead us to an order–disorder scenario of the oxygen sublattice for the structural phase transition of $LiMn_2O_4$, as previously indicated by the EXAFS study [13].

References

[1] M.M. Thackeray, Prog. Solid State Chem. 25 (1997) 1.
[2] A. Yamada, M. Tanaka, Mater. Res. Bull. 30 (1995) 715.
[3] J. Rodríguez-Carvajal, G. Rousse, C. Masquelier, M. Hervieu, Phys. Rev. Lett. 81 (1998) 4660.
[4] J. Akimoto, Y. Takahashi, Y. Gotoh, S. Mizuta, Chem. Mater. 12 (2000) 3246.
[5] J. Akimoto, Y. Takahashi, Y. Gotoh, S. Mizuta, J. Cryst. Growth 229 (2001) 405.
[6] Y. Takahashi, J. Akimoto, Y. Gotoh, K. Dokko, M. Nishizawa, I. Uchida, J. Phys. Soc. Jpn. 72 (2003) 1483.
[7] J. Akimoto, Y. Gotoh, Y. Takahashi, Solid State Ionics (in press).
[8] K. Oikawa, T. Kamiyama, F. Izumi, B. Chakoumakos, H. Ikuta, M. Wakihara, J. Li, Y. Matsui, Solid State Ionics 109 (1998) 35.
[9] G. Rousse, C. Masquelier, J. Rodríguez-Carvajal, E. Elkaim, J.-P. Lauriat, J.L. Martínez, Chem. Mater. 11 (1999) 3629.
[10] S.R. Hall, G.S.D. King, J.M. Stewart (Eds.), Xtal3.4 User's Manual, University of Western Australia, Lamb, Perth, 1995.
[11] G.M. Sheldrick, SHELX-97, University of Göttingen, Germany, 1997.
[12] A.S. Wills, I.D. Brown, VaList, CEA, France, 1999.
[13] H. Yamaguchi, A. Yamada, H. Uwe, Phys. Rev., B 58 (1998) 8.